Mesoporous Polymers Hot Paper

Deutsche Ausgabe: DOI: 10.1002/ange.201500305
Internationale Ausgabe: DOI: 10.1002/anie.201500305

Hypercrosslinked Phenolic Polymers with Well-Developed Mesoporous Frameworks**

*Jinshui Zhang, Zhen-An Qiao, Shannon M. Mahurin, Xueguang Jiang, Song-Hai Chai, Hanfeng Lu, Kimberly Nelson, and Sheng Dai**

Abstract: *A soft chemistry synthetic strategy based on a Friedel–Crafts alkylation reaction is developed for the textural engineering of phenolic resin (PR) with a robust mesoporous framework to avoid serious framework shrinkage and maximize retention of organic functional moieties. By taking advantage of the structural benefits of molecular bridges, the resultant sample maintains a bimodal micro-mesoporous architecture with well-preserved organic functional groups, which is effective for carbon capture. Moreover, this soft chemistry synthetic protocol can be further extended to nanotexture other arene-based polymers with robust frameworks.*

Mesoporous polymers with robust organic frameworks are attractive in many applications including catalysis, supports, and adsorption[1] because of their unique physicochemical properties such as high specific surface area with large pore volumes and the potential for flexible chemical modification that enables additional functionalization.[2] Until now, very few polymers with stable mesoporous frameworks have been fabricated[1,3] because of the "soft" nature of organic systems that can be highly vulnerable to collapse after template or solvent removal.[4] Therefore, it is often difficult to add nanotexture to a polymeric matrix with robust organic networks and extend the pore sizes from microporous (<2 nm) to mesoporous (2–50 nm). In this regard, it is highly desirable to strengthen the soft organic systems to enable mesopore engineering prior to template/solvent removal.[5] In addition, the strong interaction between the scaffold (templates or solvents) and the organic matrix can lead to nanoarchitecture deformations or inaccessible mesopores, giving rise to a challenge for generation of useful mesopores.[6] Addressing these issues is considered as a crucial step towards the preparation of mesoporous polymers with robust frameworks.[5,6]

Phenolic resin (PR), one of the earliest synthetic plastics, was widely adopted as the starting material for the production of many commercial products such as electrical insulators, casings and utensils.[7] More recently, it has been extensively used as a versatile precursor for the preparation of mesoporous polymers and carbons.[5,6] For example, PR oligomers or PR precursors (e.g. phenol, resorcinol, and phloroglucinol) can be easily organized by block copolymers or silica nanostructures to form mesoporous frameworks of polymer or carbon by calcination at different temperatures ranging from 350 °C to 1000 °C, thus providing a feasible strategy for the fabrication of mesoporous materials.[8] However, polymer curing and template removal generally involve post-heat treatment or concentrated sulfuric acid extraction which causes significant structural shrinkage and leaves carbonaceous bakelite frameworks with significantly reduced organic functional moieties, seriously restricting the development of mesoporous polymers.[9] In this regard, an alternative synthetic approach that can avoid or minimize framework shrinkage and preserve the functional moieties is therefore highly desirable in polymer science.

Herein, as inspired by the knowledge that PR is built from aromatic molecules, a novel synthetic strategy based on a Friedel–Crafts alkylation reaction is thus developed for the textural engineering of a PR polymer with a well-developed mesoporous framework. As illustrated in Scheme 1, the crosslinker, 1,4-bis(chloromethyl)benzene, is catalyzed to react with phenyl groups to construct the structural molecular bridges between neighboring aromatic backbones in a highly cross-linked state.[10] In nanodomains, these rigid bridges are

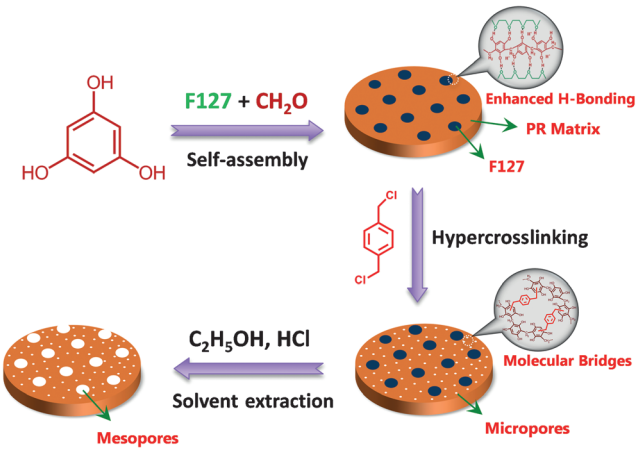

Scheme 1. Illustration of the synthetic process for Meso-PR basing on Friedel–Crafts alkylation reaction.

[*] Dr. J. Zhang, Dr. Z.-A. Qiao, Dr. S. M. Mahurin, Dr. S.-H. Chai, Dr. H. Lu, K. Nelson, Prof. S. Dai
Chemical Sciences Division, Oak Ridge National Laboratory
Oak Ridge, Tennessee, 37831 (USA)
E-mail: dais@ornl.gov
Dr. X. Jiang, Prof. S. Dai
Department of Chemistry, University of Tennessee
Knoxville, TN, 37996 (USA)

[**] This work was supported by the U.S. Department of Energy, Office of Science, Basic Energy Sciences, Chemical Sciences, Geosciences, and Biosciences Division. J.Z. thanks Dr. C. Zhang and Dr. E. Hagaman for useful discussions on NMR.

Supporting information for this article is available on the WWW underhttp://dx.doi.org/10.1002/anie.201500305.

analogous to a "steel frame" in concrete and serve to strengthen the organic matrix for robust mesopore generation, preventing pore collapse during template removal.[11] This soft synthetic protocol for polymer curing via molecular bridges, in principle, is a very useful approach to avoid the serious volume shrinkage of organic frameworks.[9] Moreover, the template removal should be also improved by the Friedel–Crafts alkylation reaction. For pristine PR, the dense, nonporous polymeric matrix prevents incorporation of any solvents into the framework, making the extraction of the triblock copolymer F127 ($EO_{106}PO_{70}EO_{106}$) (which strongly interacts with aromatic building blocks via enhanced hydrogen-bonding) very difficult.[8c] This issue can be addressed by the hypercross-linking reaction during the polymer curing process. Because the construction of rigid molecular bridges can immobilize micropores in the dense polymeric matrix,[11] the insertion of solvents for template removal is enhanced. After the complete extraction of F127 by an ethanol-HCl mixture, the resultant samples maintain a bimodal micro-mesoporous architecture with robust organic frameworks, which exhibit the structural advantages of microporous materials and mesoporous materials.[12] As expected, these polymers with hierarchical pores are particularly useful for gas adsorption, separation, and catalysis.[13] Experimentally, the final samples are denoted as Meso-PR-X, where X (0, 12, 24, 36, 48) refers to the number of hours of Friedel–Crafts alkylation reaction. The detailed synthetic procedure is provided in the Experimental Section (see Supporting Information).

Textural information of the Meso-PR polymers was obtained from N_2-sorption isotherms. In Figure 1 a, a type IV curve featuring a pronounced hysteresis loop is observed for Meso-PR-X (X = 12, 24, 36 and 48), clearly suggesting the presence of accessible mesopores in the polymeric matrices.[8] Evidently, the mesoporosity of Meso-PR-X is closely dependent on the reaction time of the hypercrosslinking process, indicating that the amount of micropores is a crucial factor in the extraction of templates with accessible mesopore space (Table 1). For example, it is very difficult to remove the F127 molecules in Meso-PR-0 due to the absence of micropores in its organic networks. The mesoporous structure develops rapidly with prolonged cross-linking time to increase the microporosity in the PR matrix (Table 1)[10,11] and well-defined mesopores are obtained when the reaction time reaches 36 h (Figure 1 b). Further extending the reaction time results in a slight decrease of the mesopore surface area (S_{meso}) and an enlargement of the mesopores as seen in the appearance of a shoulder in the pore size distribution (Figure 1 b). The specific surface area of sample Meso-PR-36 is measured to be 782 $cm^2 g^{-1}$, by taking advantage of the structural benefits of bimodal micro-mesoporous materials.[12] Note that the corresponding S_{meso} of Meso-PR-36 is calculated as 481 $m^2 g^{-1}$, highly comparable to the value (450 $m^2 g^{-1}$) of Meso-PR-350 that was synthesized by calcination at 350 °C to pyrolyze F127 templates. This finding clearly demonstrates that the structural template, triblock copolymer F127, has been completely removed by solvent extraction, demonstrating the importance of microporosity in the generation of mesopores.

Table 1: Porous properties of Meso-PR polymers.

Polymer	S_{total}[a] [$m^2 g^{-1}$]	S_{micro}[b] [$m^2 g^{-1}$]	S_{meso}[c] [$m^2 g^{-1}$]	PD_{meso}[d] [nm]	PV[e] [$cm^3 g^{-1}$]
Meso-PR-0	< 1	–	< 1	–	–
Meso-PR-12	157	39	118	7.2	0.16
Meso-PR-24	287	104	183	8.2	0.22
Meso-PR-36	782	301	481	8.2	0.68
Meso-PR-48	757	328	429	8.5	0.68
Meso-PR-350	474	24	450	7.0	0.66

[a] Total surface area. [b] Microporous surface area calculated from *t-plots*. [c] Mesoporous surface area. [d] Mesoporous pore diameter. [e] Pore volume.

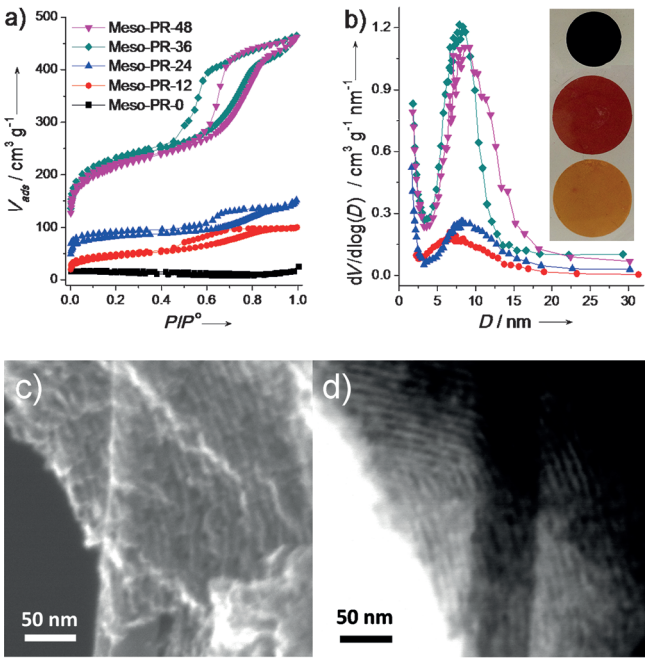

Figure 1. Textural characterization of Meso-PR samples. a) N_2-sorption isotherms. b) pore size distribution plots. c) SEM image. d) TEM image. Inset (b) is the photograph of Meso-PR-350, Meso-PR-36 and pristine PR (from top to bottom), and the diameter of pristine PR is measured as 13 mm.

The other advantage of the soft chemistry synthetic approach is the efficient reduction of serious skeleton shrinkage, which can be clearly demonstrated through visual observation. In Figure 1 b inset, no apparent change in the diameter is observed between pristine PR and Meso-PR-36. In contrast, the diameter of Meso-PR-350 obviously decreases from 13 mm to 9.3 mm, displaying evident thermal-induced volume contraction. This comparison indicates that the serious structural shrinkage that occurs during the polymer curing and template removal processes has been addressed by hypercrosslinking the organic matrix with rigid molecules. Such morphology differences on the macroscale (mm) are closely related to the porous structure evolution in the nanoscale (nm). In Figure S1 (Supporting Information), the pore size distribution plot of Meso-PR-350 shows a moderate decrease in peak position compared to the

Meso-PR-36 polymer, suggesting that considerable pore narrowing happens during thermal treatment. The corresponding mesopore size is determined to be 7.0 nm and 8.2 nm for Meso-PR-350 and Meso-PR-36, respectively (Table 1). These larger mesopores indicate that the framework shrinkage of the PR matrix is efficiently suppressed in Meso-PR-36, highlighting the advantage of our synthetic approach in nanotexturing of soft organic systems.

The nano-morphology of Meso-PR-36 polymer was imaged by scanning transmission electron microscopy (STEM). Using scanning electron microscopy (SEM), a typical mesoporous morphology with regular, ordered surface intervals is observed for Meso-PR-36, indicating the successful extraction of F127 from the polymeric matrix (Figure 1c).[4a] More detailed information about this nanostructure can be revealed using transmission electron microscopy (TEM). In Figure 1d, the mesochannels as indicated by the bright lines passing through the PR matrix are arranged in a regular pattern, and their corresponding diameter is measured to be approximately 8.0 nm, comparable to the value obtained from N_2-sorption isotherms (Table 1).[8] In Figure S2, this porous structure is further demonstrated by the X-ray diffraction (XRD) pattern, where intense reflections of mesoporous frameworks with pore diameter ca. 7.9 nm are observed for Meso-PR-36.[8c] It should be pointed out that the slight difference in mesopore size (8.2 nm vs. 8.0 nm vs. 7.9 nm) obtained from N_2-sorption, TEM image and XRD pattern, can be attributed to the methods used for calculation.

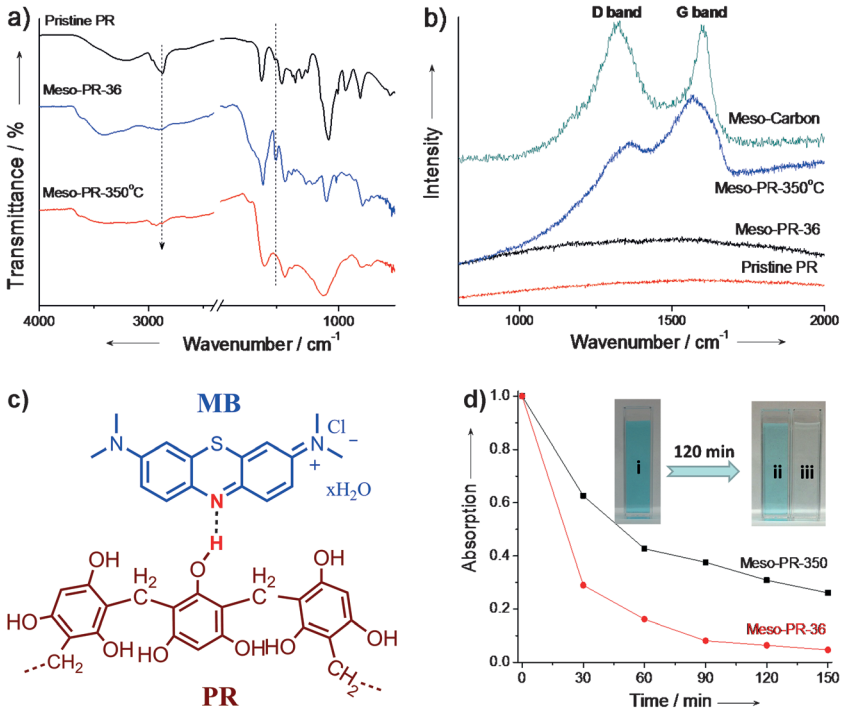

Figure 2. Framework characterization of Meso-PR polymers, together with pristine PR and Meso-Carbon as reference samples. a) FT-IR spectra. b) Raman spectra. c) hydrogen bonding between MB and phenolic-OH. d) MB concentration in aqueous solution as a function of time. Inset (d) is the photograph of MB solution, where i, ii and iii correspond to the starting MB solution, the MB solution obtained from Meso-PR-350, and Meso-PR-36.

The chemical structure of the Meso-PR polymers was characterized by Fourier-transform infrared (FT-IR), solid-state ^{13}C nuclear magnetic resonance (NMR), and Raman spectroscopy. In Figure 2a, the featured bands assigned to typical PR polymers are observed for Meso-PR-36, such as the stretching vibration of phenolic-OH groups at 3400 cm^{-1}, the absorption bands of aromatic =C–H and C=C at 3000 cm^{-1} and 1610 cm^{-1}, and the bending vibration of saturated CH_2 at 1440 cm^{-1}.[9,14] These results suggest high preservation of the PR chemical structure in Meso-PR-36. The successful cross-linking of aromatic 1,4-bis(chloromethyl)benzene in the polymeric matrix as molecular bridges enhances the absorbance at 1505 cm^{-1}, which originates from C=C groups in the aromatic rings.[15] For NMR characterization (Figure S3), the broad bands should be categorized as two carbon species, that is, the aliphatic carbons assigned to methylene bridges (10–50 ppm) and the aromatic carbons contained in the phenyl rings (90–160 ppm), again indicating a well-preserved PR networks.[8b] Compared with pristine PR, the evident quenching of the C–H stretch from the F127 triblock copolymer at 2900 cm^{-1} is another indicator of the successful removal of the templates in Meso-PR-36.[9,14] Due to the partially carbonaceous nature of the polymeric frameworks and significant elimination of organic functional moieties (such as phenolic-OH groups), the characteristic stretching modes of PR polymers become broader and less resolved in Meso-PR-350,[9,14] again underlining the advantage of the soft chemistry protocol for mesoporous PR synthesis. Figure 2b displays the Raman spectra of resultant samples. Quite different from the spectra of Meso-PR-36 and pristine PR, evident G and D bands at 1580 cm^{-1} and 1360 cm^{-1} with an intensity ratio (I_G/I_D) of 1.3 are observed on Meso-PR-350, clearly suggesting that the organic network is indeed partially carbonized by thermal treatment during F127 pyrolysis.[16] This finding is in good agreement with the results of FT-IR characterization. As shown in Figure 2c, preservation of the polymeric framework in Meso-PR-36 with abundant phenolic-OH groups bound to pore surfaces can be easily probed using a dye absorption experiment.[17] It has been reported that methylene blue hydrate (MB) dye with a nitrogen-containing aromatic ring can selectively interact with phenolic-OH groups through strong hydrogen bonding, making it a suitable reagent for -OH detection.[17a] In Figure 2d, a faster absorption rate and greater dye adsorption is observed for Meso-PR-36 compared to Meso-PR-350, clearly indicating that more -OH groups are present in the former polymeric network.[17] Finally, the organic network of Meso-PR has been well preserved simply by employing the soft chemistry synthetic strategy for sample preparation, which should be an effective approach to further functionalize mesoporous polymers for target-specific applications.[2]

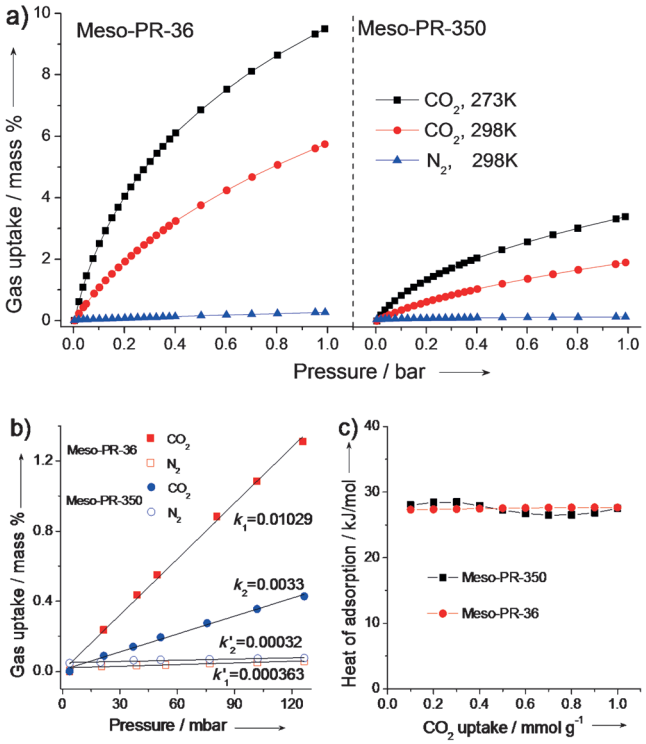

Figure 3. Gas absorption performance of Meso-PR-36 and Meso-PR-350. a) CO_2 and N_2 isotherms at 273 K and 298 K. b) Initial slope calculation for CO_2 and N_2 isotherms collected at 298 K. c) Isosteric heat of absorption for CO_2 at different loadings.

Figure 3 displays the gas adsorption performance of Meso-PR-36 and Meso-PR-350. The CO_2 uptake of Meso-PR-36 at 273 K and 298 K is determined as 9.5 wt.% and 5.8 wt.% under 1.0 bar CO_2 pressure. In comparison, these values are much higher than those obtained from Meso-PR-350, where only 3.4 wt.% and 1.9 wt.% CO_2 capacities are measured at 273 K and 298 K, respectively. This improved CO_2 capture capacity, presumably, can be attributed to the abundant micropores,[12,13] which were generated by the rigid molecular bridges for solvent extraction of F127 templates. That is, the incorporation of micropores on the mesopore walls is not only beneficial for template removal, but can also enhance the functionality of the mesoporous materials, such as improved gas storage capabilities.[13] In addition, this unique bimodal pore structure with interconnected micro- and mesopores, in principle, can avoid the mass diffusion limitations associated with very small pores and make every micropore easily accessible to guest molecules, both of which are favorable for CO_2 capture.[12,13] To better illustrate this structural benefit, a PR polymer with predominant microporous structure is selected as a reference sample (Figure S4). In Figure S5, the CO_2 capture capacity at 273 K and 298 K is determined as 7.3 wt.% and 5.1 wt.%, still lower than the values of Meso-PR-36, despite having a similar microporous surface area (323 $m^2 g^{-1}$ vs. 301 $m^2 g^{-1}$). Furthermore, this structural advantage can also be demonstrated by our previous study, whereas the microporous polymer TFM-1 with a surface area of 738 $m^2 g^{-1}$ shows a CO_2 uptake capacity of 7.6 wt.% at 273 K.[18] The CO_2 separation performance was evaluated by N_2 absorption experiment. By linear fitting the CO_2 and N_2 uptake curves at low pressure (< 0.2 bar), the ideal CO_2/N_2 absorption selectivity is calculated as 28 and 10 for Meso-PR-36 and Meso-PR-350, respectively, indicating that Meso-PR-36 has a higher selectivity towards CO_2 (Figure 3b). To the best of our knowledge, this enhanced CO_2 separation performance can be attributed to the abundant micropores, rather than the dipole–quadrupole interaction[12,13] because no evident difference in the isosteric heat of absorption was measured between Meso-PR-36 and Meso-PR-350 (Figure 3c). Hence, a better CO_2 capture performance is obtained on Meso-PR-36, owing to the unique structural benefits of the bimodal micro-mesoporous framework.

In conclusion, a soft chemistry synthetic strategy designed to avoid serious framework shrinkage and preserve the organic functional moieties has been successfully developed based on Friedel–Crafts alkylation reaction for the nanotexturation of PR matrix with well-developed mesoporous frameworks. The construction of structural molecular bridges between neighboring aromatic backbones in a highly crosslinked state, not only strengthens the soft organic system to enable mesoporous engineering, but also creates abundant micropores for the inclusion of solvents for template removal. Benefiting from the synthetic protocol, the resultant sample is a bimodal micro-mesoporous material with a robust organic framework, which exhibits a promising property for CO_2 capture. Currently, this synthetic method is being employed for the fabrication of polystyrene based nanoarchitectures, by taking advantage of the molecular bridges for polymeric curing and template removal. We believe that this soft chemistry synthetic protocol can be further extended to the nanotextural engineering of other aromatic based polymers.

Keywords: CO_2 capture · friedel–crafts alkylation · hypercrosslinking · mesoporous frameworks · phenolic polymer

How to cite: *Angew. Chem. Int. Ed.* **2015**, *54*, 4582–4586
Angew. Chem. **2015**, *127*, 4665–4669

[1] a) S. A. Johnson, P. J. Ollivier, T. E. Mallouk, *Science* **1999**, *283*, 963; b) X. Wang, K. Maeda, X. Chen, K. Takanabe, K. Domen, Y. Hou, X. Fu, M. Antonietti, *J. Am. Chem. Soc.* **2009**, *131*, 1680; c) F. Liu, W. Kong, C. Qi, L. Zhu, F.-S. Xiao, *ACS Catal.* **2012**, *2*, 565; d) D. Chandra, B. K. Jena, C. R. Raj, A. Bhaumik, *Chem. Mater.* **2007**, *19*, 6290; e) W. Wang, H. Wang, W. Wei, Z.-G. Xiao, Y. Wan, *Chem. Eur. J.* **2011**, *17*, 13461; f) Y. Zhang, S. Wei, F. Liu, Y. Du, S. Liu, Y. Ji, T. Yokoi, T. Tatsumi, F.-S. Xiao, *Nano Today* **2009**, *4*, 135.

[2] a) F. Liu, L. Wang, Q. Sun, L. Zhu, X. Meng, F.-S. Xiao, *J. Am. Chem. Soc.* **2012**, *134*, 16948; b) Y. Yue, R. T. Mayes, J. Kim, P. F. Fulvio, X.-G. Sun, C. Tsouris, J. Chen, S. Brown, S. Dai, *Angew. Chem. Int. Ed.* **2013**, *52*, 13458; *Angew. Chem.* **2013**, *125*, 13700; c) Z. Yang, J. Wang, K. Huang, J. Ma, Z. Yang, Y. Lu, *Macromol. Rapid Commun.* **2008**, *29*, 442.

[3] a) P. Kuhn, A. Forget, D. Su, A. Thomas, M. Antonietti, *J. Am. Chem. Soc.* **2008**, *130*, 13333; b) J. Jang, J. Bae, *Chem. Commun.* **2005**, 1200; c) R. Dawson, F. Su, H. Niu, C. D. Wood, J. T. A. Jones, Y. Z. Khimyak, A. I. Cooper, *Macromolecules* **2008**, *41*, 1591; d) D. Chandra, A. Bhaumik, *J. Mater. Chem.* **2009**, *19*, 1901; e) K. Kailasam, Y.-S. Jun, P. Katekomol, J. D. Epping, W. H. Hong, A. Thomas, *Chem. Mater.* **2010**, *22*, 428.

[4] a) J. Zhang, F. Guo, X. Wang, *Adv. Funct. Mater.* **2013**, *23*, 3008; b) N. Li, M. Zheng, S. Feng, H. Lu, B. Zhao, J. Zheng, S. Zhang, G. Ji, J. Cao, *J. Phys. Chem. C* **2013**, *117*, 8784.
[5] I. Muylaert, A. Verberckmoes, J. De Decker, P. Van Der Voort, *Adv. Colloid Interface Sci.* **2012**, *175*, 39.
[6] Y. Wan, Y. Shi, D. Zhao, *Chem. Mater.* **2008**, *20*, 932.
[7] W. Hesse, J. Lang, *Ullmann's Encyclopedia of Industrial Chemistry*, Wiley-VCH, Weinheim, **2000**.
[8] a) C. Liang, K. Hong, G. A. Guiochon, J. W. Mays, S. Dai, *Angew. Chem. Int. Ed.* **2004**, *43*, 5785; *Angew. Chem.* **2004**, *116*, 5909; b) Y. Meng, D. Gu, F. Zhang, Y. Shi, H. Yang, Z. Li, C. Yu, B. Tu, D. Zhao, *Angew. Chem. Int. Ed.* **2005**, *44*, 7053; *Angew. Chem.* **2005**, *117*, 7215; c) C. Liang, S. Dai, *J. Am. Chem. Soc.* **2006**, *128*, 5316; d) F. Zhang, Y. Meng, D. Gu, Y. Yan, C. Yu, B. Tu, D. Zhao, *J. Am. Chem. Soc.* **2005**, *127*, 13508; e) J. Liu, T. Yang, D.-W. Wang, G. Q. (Max) Lu, D. Zhao, S. Z. Qiao, *Nat. Commun.* **2013**, *4*, 2798.
[9] X. Zhuang, X. Qian, J. Lv, Y. Wan, *Appl. Surf. Sci.* **2010**, *256*, 5343.
[10] M. Rueping, B. J. Nachtsheim, *Beilstein J. Org. Chem.* **2010**, *6*, 6.
[11] S. Xu, Y. Luo, B. Tan, *Macromol. Rapid Commun.* **2013**, *34*, 471.
[12] R. M. Dorin, H. Sai, U. Wiesner, *Chem. Mater.* **2014**, *26*, 339.
[13] a) Z. Xin, J. Bai, Y. Shen, Y. Pan, *Cryst. Growth Des.* **2010**, *10*, 2451; b) A. P. Katsoulidis, M. G. Kanatzidis, *Chem. Mater.* **2012**, *24*, 471.
[14] a) B. You, J. Yang, Y. Sun, Q. Su, *Chem. Commun.* **2011**, *47*, 12364; b) W. Wang, X. Zhuang, Q. Zhao, Y. Wan, *J. Mater. Chem.* **2012**, *22*, 15874.
[15] C. F. Santa, L. Sierra, *J. Braz. Chem. Soc.* **2011**, *22*, 2312.
[16] J. Schuster, R. Köhn, A. Keilbach, M. Döblinger, H. Amenitsch, T. Bein, *Chem. Mater.* **2009**, *21*, 5754.
[17] a) H. Kosonen, S. Valkama, A. Nykänen, M. Toivanen, G. ten Brinke, J. Ruokolainen, O. Ikkala, *Adv. Mater.* **2006**, *18*, 201; b) S. Valkama, A. Nykänen, H. Kosonen, R. Ramani, F. Tuomisto, P. Engelhardt, G. ten Brinke, O. Ikkala, J. Ruokolainen, *Adv. Funct. Mater.* **2007**, *17*, 183.
[18] X. Zhu, C. Tian, S. M. Mahurin, S.-H. Chai, C. Wang, S. Brown, G. M. Veith, H. Luo, H. Liu, S. Dai, *J. Am. Chem. Soc.* **2012**, *134*, 10478.

Received: January 13, 2014
Published online: February 12, 2015

